ESSAY

The Hessdalen Lights Seen as the Aerial Counterpart of an Unsuspected Subsoil Phenomenon. Is the Earth Harboring a Multimouth Wormhole?

Gianni Pascoli

pascoli@u-picardie.fr

orcid.org/0000-0002-4923-0961

Université de Picardie Jules Verne (UPJV)

HIGHLIGHTS

Certain types of mysterious aerial lights reported around the world might be caused by a small particle wormhole deep in the location's subsoil.

ABSTRACT

To date, Hessdalen lights (HLs) are misunderstood; nevertheless, these phenomena are surprisingly ignored by most of the scientific community. However, a few researchers, such as Erling Strand and Massimo Teodorani, have paved the right path by showing that experimental methods of physics can be applied to study HLs. Additionally, we believe that matter cannot simply be brushed aside and that it deserves a serious examination. Recently, we proposed a possible origin of HLs (Pascoli, 2021). The basic idea—a micrometric wormhole manifestation—is promoted here, and we suggest that the Hessdalen-type lights, seen pretty much everywhere in the world, may eventually be interpreted as a symptom of an unsuspected phenomenon deep in the subsoil of the considered site. The idea of a geological origin for the Hessdalen lights has already been proposed (Teodorani, 2004, 2014); however, this interesting suggestion is being reconsidered from an entirely new perspective. The present paper has to be seen as a working hypothesis, in which the main interests are to foster thinking on underlying physics and to suggest a full series of experiments that can be performed on these very enigmatic Hessdalen lights. Regardless of the strength of a hypothesis, the experiment is the final arbiter in science.

KEYWORDS

Hessdalen, wormhole, photoionization, model, magnetic field, magnetic monopole, ultrasound, geology, volcanism.

INTRODUCTION

In general, we believe traversable wormholes exist only in science-fiction movies.[1] Thus, so far, no one has proposed a method for large wormholes to form; without the hypothetical ingredient of negative mass or other phantom matter, wormholes are consubstantially unstable and not traversable within the strict framework of general relativity (Morris & Thorne, 1988; Blazquez-Salcedo, Knoll

and Radu, 2021 and references therein). In contrast, we know that these types of objects have naturally existed at the very beginning of the Universe, even though quantum fluctuations at the Planckian scale. In the very early (quantum) stage, the Universe should have a foam-like topological structure. The possibility thus exists that the inflationary phase has provided a natural mechanism for increasing such wormholes to a macroscopic size (Frolov

Figure 1. Illustration of galaxies (National Aeronautics and Space Administration (NASA)/European Space Agency (ESA) Hubble Space Telescope) connected from center to center by a wormhole, according to Dai and Stojkovic (2019, 2020).

& Novikov, 1998; Kirillov & Savelova, 2011). Admittedly, the question regarding the stability of wormholes is undoubtedly beyond the domain of general relativity. However, within other, more extended contexts, solutions for stable and even traversable wormholes have been tested. Gao, Jafferis, and Wall (2017) have emitted the hypothesis that quantum entanglement would provide an exotic ingredient needed for the stability of wormholes. Iqbal and Ross (2022) have attempted to construct traversable wormhole solutions using the negative Casimir energy. However, as recognized by the latter authors, the major conundrum is that it is very difficult to build wormholes larger than 10^{-21} m ! The existence of large, stable, traversable wormholes is not, however, definitely excluded (Maldacena & Milekhin, 2021; Blazquez-Salcedo, Knoll & Radu, 2021).

Thus, despite theoretical difficulties, an increasing number of astrophysicists believe that macroscopic wormholes could be existing in the real world. Wormhole gas that simulates dark matter has been envisioned (Kirillov & Savelova, 2011). Likewise, researchers have examined the possible existence of wormholes in the bulge and halo of the Milky Way (Rahaman et al., 2014; Bakopoulos et al., 2022; Das and Kalam, 2022). In addition, extradimensional connections between galaxies have been suggested repeatedly. In particular, some authors have questioned if the Milky Way center can reside in a wormhole instead of a black hole with its unwanted central point singularity (Dai & Stojkovic, 2019, 2020; Krasnikov, 2020). If a wormhole mouth indeed exists at the galactic center, the Milky Way could be connected to another very distant galaxy (Fig.1).

Figure 2. *Stars connected from center to center by a wormhole, according to Dzhunushaliev et al. (2011).*
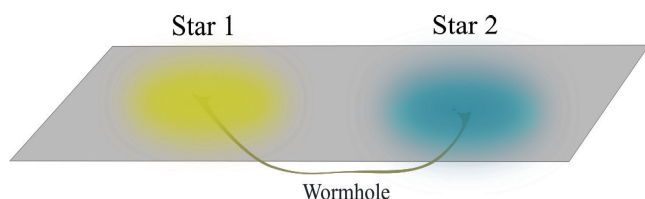
Wormhole Connecting Two Stars

The case of two stars connected by a wormhole has also been examined (Dzhunushaliev et al., 2011). By following these authors, assuming first that stable wormholes exist in the galaxy, we can imagine that the mouths of these wormholes can act as condensation nuclei for the stars. In this case, the evolution of the two components of a binary stellar system would not only be influenced by the apparent gravitational forces between them but also by an extradimensional bridge connecting their central regions (Fig. 2).

If the existence of a galactic or a stellar wormhole is proven one day, we expect that there will likely be many types, most of which are microscopic or nanoscopic in size.[2] However, all the researchers quoted above attempt to find these exotic entities in very remote locations, whereas some of them may be at our fingertips. Especially Pascoli (2021) suggested that Hessdalen lights (HLs) can eventually be a manifestation of microscopic wormholes. We continue this idea here from an extended point of view, considering that, generally, some big ball lighting phenomena (BBLs) seen around the world could be explained by similar mechanisms.

Extradimensional Connection Between the Center of the Sun and the Center of a Planet in the Solar System

Is there an extradimensional connection between the center of the Sun and the center of a planet (the Earth) in the solar system? This idea is entirely speculative; however, it directly results from the suggestion made by Dzhunushaliev et al. (2011) regarding the connection of two stars by a wormhole. An important and obvious difference is that a planetary wormhole must be absolutely tiny compared to a stellar wormhole. By considering this statement, the question is then: What could be the maximal size of the mouth of the corresponding wormhole?

Gravity and Wormholes

Even though the question in itself deserves a deep examination (cf. note 2), we can consider that a wormhole and a black hole defined by the same mass parameter grossly produces gravitational effects of the same order of magnitude in the surrounding region. This point is illustrated by the fact that it is often difficult to know if we are handling a wormhole or a black hole (Dai & Stojkovic, 2020; Krasnikov, 2020).

Thus, for a star, the characteristic size, R_{WH}, of the mouth of the central wormhole can be approximately estimated by using the following relationship:

$$R_{WH} \sim R_{Schwarzchild} = \frac{2\,GM_{BH}}{c^2} \tag{1}$$

Where M_{BH} is the mass of the equivalent black hole, c is the speed of light, and G is the gravitational constant. We know the stability conditions of a star of a given mass. Then, it appears natural to admit that a hypothetical black hole or wormhole located at the center of a star necessarily has a mass much smaller than that of the host star, let $M_* \sim 2\ 10^{30}\ kg$. The condition is then:

$$M_{BH} \ll M_* \tag{2}$$

With (1), we obtain $R_{WH} \ll 1\ km$. Let us examine now the same situation but related to a planet. For the Earth, the mass is $\sim 6\ 10^{24}\ kg$. In this case, the largest size of the mouth of a hypothetical central wormhole is $R_{WH} \ll 10\ mm$.

Eventually, in the following paragraphs, our starting base is the existence of a Sun–Earth wormhole, assimilated to a microscopic channel allowing the passage of solar radiation and magnetic field but not traversable by matter. In addition, let us specify that the wormhole under consideration is assumed to connect two regions of space with a null gravitational field (the center of the Sun and the center of the Earth).

Heating the Inner Earth

The preceding result, based on very crude considerations, provides only a maximum radius. However, we must still drastically minimize this radius for geological reasons. It is well known that the external heat source of the Earth is the Sun. Energy from the Sun is transferred through space, passes through the Earth's atmosphere, and reaches the Earth's surface. However, the Earth is also heated from the inside, as attested by volcanism and plate tectonics. The sources are well known and listed: i. the radiogenic heat produced by the radioactive decay of isotopes, such as ,^{235}U, ^{238}U, ^{232}Th, and ^{40}K, dispersed in the mantle and crust; ii. the residual heat from when our planet was first formed; and iii. various minor processes, such as tidal deformation and chemical segregation (Lay, Hernlund, & Buffett, 2008). Based on the arguments presented above, if the center of the Sun and that of the Earth are connected by an extradimensional path, another contributing source to the inner heating of the Earth could now come from a "mini-sun" located at its center, feeding it in energy.

Nevertheless, it seems that no place exists for a potentially detectable mini-sun because the value of the heat flux that comes from inside the Earth is well known,
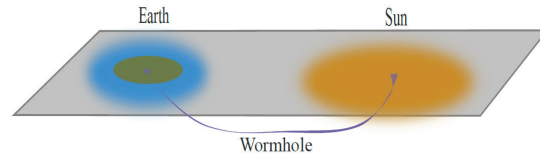

Note. This figure is the same as Figure 2; however, in Figure 2, the wormhole is kilometric in size (here the size refers to the approximate dimension of the wormhole mouths, measured by an outer observer), whereas it is necessarily micrometric in size for a planetary wormhole

Figure 3. Hypothetical permanent microscopic wormhole connecting the center of the Sun and the center of the Earth.

and its sources are clearly identified. Then, we must imperatively impose a strong constraint on the magnitude of the power emitted by this mini-sun to make it undetectable. The flow of heat from the Earth's interior to the surface is estimated at $5\ 10^4\ GW$ (Davies & Davies, 2010). While the Earth's surface heat flow is well measured, the various energy sources, such as radiogenic heating, secular cooling of the mantle, and heat flow from the core, are relatively poorly estimated by the models (The KamLAND Collaboration, 2011; Dye, 2012; Ruedas, 2017; Sammon & McDonough, 2022). Possibly the uncertainty in the models may increase to one-twentieth of the Earth's internal heat budget (Davies & Davies, 2010)**.** However, to be in agreement with future and more refined geoneutrino measurements**,** we have chosen to take a value largely smaller than $10^3\ GW$ as an estimate of the corresponding uncertainty. This allows us to fix an upper limit for the size R_{WH} of the mouth of the central wormhole. By assimilating the mouth of this wormhole to a spherical black body of radius R_{WH} and with a temperature of $T_{WH} = T_S = 10^7\ K$, we can apply the well-known relationship:

$$P_{WH} = 4\pi\ \sigma\ R_{WH}^2 T_{WH}^4 \tag{3}$$

Figure 4. Multibranched wormhole (inspired from Emperan et al., 2021)
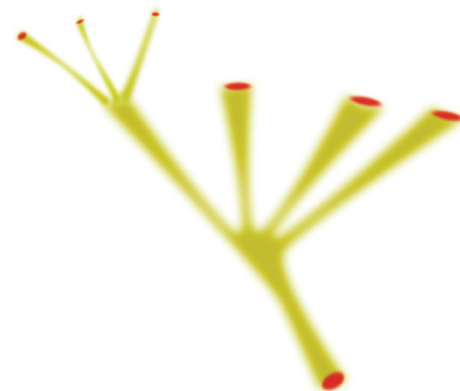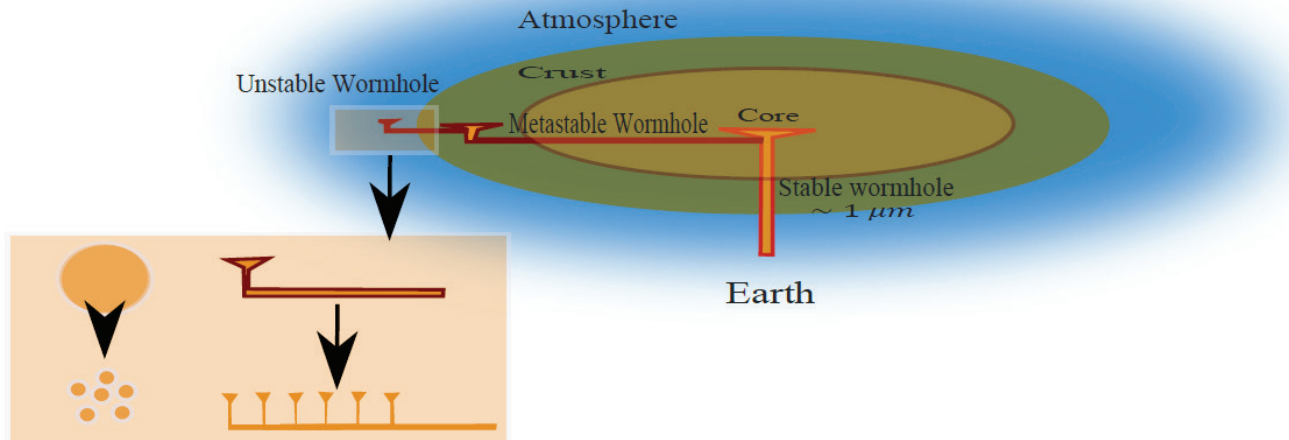
Note. This figure displays an architecture from the unique micrometric central wormhole (size < 10^{-5} - 10^{-6} m) to an unstable nanometric wormhole emerging in the atmosphere over a given site (the Hessdalen valley, for instance or still elsewhere.

Figure 5. Illustration of a possible hierarchy of wormholes in the Earth

where the Stefan–Boltzmann constant σ = 5.67 10^{-8} $W\,m^{-2}\,K^{-4}$. We immediately deduce that $R_{WH} \leq 10^{-5}$ - 10^{-6} m. . We conclude that such a wormhole can easily reside at the center of the Earth in a permanent manner, i.e., since its formation 4.54 billion years ago (Fig. 3). Obviously, the condition that the size of the wormhole is microscopic is a prerequisite to satisfy both the gravitational criterion limiting the associated gravitational mass and, above all, the strong constraint imposed by the heat flow measurements. By considering these conditions, the presence of a wormhole of micrometric size at the Earth's center can remain unsuspected.

We start with the idea that a microscopic and undetectable wormhole mouth is readily present at the center of the Earth. However, a microscopic wormhole can be perceived as a fluctuating entity, and multiple branches can emerge from this central and permanent mouth. These branches can be formed from the division of the mouth. The idea of multimouth wormholes has been very

recently proposed and analyzed from a mathematical point of view by Emperan et al. (2021). Following these authors, it is possible to construct multi-mouth wormholes sufficiently long-lived to be traversable, even if detailed investigations are needed. Figure 4, which shows this division, is taken from this very interesting paper. A good image is that of a tree, with a trunk (a permanent wormhole connecting the center of the Sun and the center of the Earth) and branches connecting the trunk to another point in the subsoil of a given place in the Earth, from which a very tiny wormhole (seen here as the primary source of an aerial BBL) sporadically emerges into the atmosphere. This emerging entity will be termed a seed in what follows (see Fig. 6).

Hessdalen: Special or Accidental BBL Site?

In a preceding paper (Pascoli, 2021), we discussed this important question to determine whether the Hessdalen Valley is a special or an accidental BBL site. We have imagined that the space is a kind of topological porous medium, of which we distinguish only three spatial dimensions (the smooth surface of the porous medium). The wormhole can then percolate in a purely accidental manner toward a specific point and, for a finite moment (a few years), i.e., in the present situation at Hessdalen. Figure 2 of the abovementioned paper exhibits a direct connection between any area taken in the Sun and the Hessdalen valley. This view is obviously oversimplistic, as presented for illustrative purposes. Herein, it is up to us to specify the details of the mechanism.
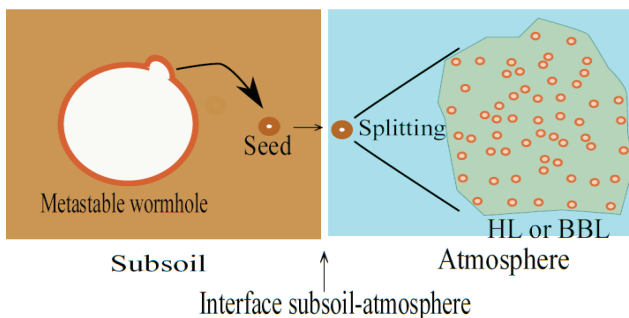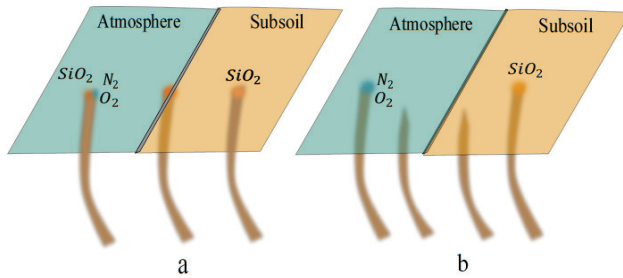

Figure 6. Metastable wormhole producing an embryonic entity (a seed) of a BBL

Note. **Fig. 7a.** *Direct apparition through the interface subsoil atmosphere. In this case, an observer can see the BBL erupting from the subsoil with a rising plum of molten tiny silicon clusters. Fig. 7b. Apparition by retraction. In this second scenario, the wormhole appears instantaneously in the atmosphere, and only the air molecules are ionized. Then the observer sees the BBL suddenly popping up in the middle of the sky.*

Figure 7. Apparition Modes of an HL Into the Atmosphere

In the present scenario, we imagine a fluctuation appearing from the main permanent wormhole mouth at the center of the Earth. This fluctuation creates a new wormhole mouth that can appear anywhere inside the Earth; then, this mouth rises to the surface, where rare offshoots can emerge, eventually producing a visible aerial phenomenon known as a BBL (Fig. 5).

A direct analogy can be made with volcanism, where a hot spot rises from deep within the Earth. In a more precise manner, we first imagine that the fluctuation issued from the central and permanent wormhole mouth creates a metastable wormhole mouth that is fixed somewhere under the surface at a given site. This site can be located anywhere, but accidentally we can assume that this one is today situated deep just under the Hessdalen valley. Let us note that it is not fully excluded that the emer-

Table 1. Synoptic Table of the Wormhole Types

Wormhole Type	Size	Number	Lifetime
Central	~1 μm ($P \sim 1\ GW$)	1	~5x 10^9 years
Metastable Underground	~10 nm ($P \sim 1\ MW$)	1000	~100–1000 years
Unstable Atmospheric	~1 nm ($P \sim 10\ kW$)	> 1 following the observations	~1 second–1 hour

Note. The numbers in this table are provided purely as an indication only. The characteristic sizes of the wormhole mouths are approximately scaled to the emitted powers. The central wormhole (P= 1 GW) can simultaneously feed 1000 metastable wormholes (P = 1 MW) distributed all across the world. The central wormhole is assumed to be permanent. Each of the metastable wormholes is assumed to reside in the underground of a defined area (for instance the Hessdalen valley) for a duration of a few centuries.

gence of this metastable mouth located just under the free surface of the Earth could possibly result from the geological nature of the site under question. We know that Hessdalen lights have been mostly frequent over the period between 1981 and 1984, even though the phenomenon existed before and still exists today; however, it is far less frequent. The phenomenon will probably disappear in a few decades and show up elsewhere. For the time being, we can reasonably propose the idea that an active HL (or more generally BBL) "tank", similar to a magma chamber in the volcanism domain, was present deep under the Hessdalen valley for a few hundred years; this "tank" was very active between 1981 and 1984 and is far less active now (the analogy with volcanism seems to be very strong and can help us understand the phenomenon). We then have the following hierarchy (inspired from the paper of Emperan et al., 2021):

i. A stable wormhole mouth at the center of the Earth with a radius of 1~μm for a power of the order of 1 GW.

ii. A metastable wormhole mouth situated deep below the Hessdalen site with a radius of ~3 $10^{-8}\ m$ for a power of 1MW. This metastable wormhole mouth is assimilated to a "tank" from which a seed of~ $10^{-9}\ m$ occasionally emerges. Then, this seed passes through the intersurface soil-atmosphere and becomes visible by the photoionization of the ambient air.

iii. A swarm of unstable and very tiny wormhole mouths globally forming the skeleton of a BBL. This skeleton is obtained from the division of the seed. In the swarm, the individual units successively appear, divide, and retract within a time scale of the order 10^{-4}- $10^{-3}\ s$. However, these individual units remain correlated. The time scale is derived from the results presented in the paragraph 6, and it can persist between these very sudden phases over a few seconds, minutes or hours. The swarm of very tiny correlated wormholes is randomly fed by the metastable wormhole mouth presumably located under the Hessdalen valley to date (maybe a few kilometers deep) (Fig. 6 and Table 1).

The Hessdalen valley covers an area of approximately 1.5 $10^7\ m^2$ (15 km x 1 km). By assuming that the metastable wormhole mouth is 10 km under the site of the Hessdalen Valley and this mouth radiates in an isotropic manner, we find excess heat flow of ~15 $mW\ m^{-2}$ at a surface under the Hessdalen site. On the other hand, the mean flow at the surface of the Earth is estimated to be 65 $mW\ m^{-2}$ over the continental crust (Pollack et al., 1993; Fuchs *et al.,* 2021). It would be interesting to measure this

flow in the subsoil of the Hessdalen valley, and to compare it to the flow in the surrounding areas, to see if the ground heat flux is not slightly higher in the Hessdalen valley than in the surrounding areas. The measurement of the flow would allow us to estimate the depth of a hypothesized metastable wormhole. In fact, even after these measurements are realized and yielding a hopeful outcome, we could still legitimately claim that it is not a wormhole but, rather, that an unknown source of energy is hidden in the subsoil of the Hessdalen valley. In this case, measuring the ground heat flux could nonetheless be very positive for understanding HLs.

Transition Subsoil-Atmosphere

A wormhole branch moving from the BBL "tank" can pass across the interface subsoil-atmosphere by using two different modes. First, this passage can be direct, and a diffuse plasma of silicate matter can be driven by the wormhole mouth (Fig. 7). In this case, the presence of silicon and magnesium/calcium ions should be detectable in the spectra of BBLs.[3]. In the second situation, the wormhole can retract and reach the atmosphere without truly crossing the interface. Then, the BBL must be exclusively composed of atmospheric gas (dinitrogen and dioxygen). It would be interesting to know the relative probability of a direct crossing against an underground air transition without crossing.

Number of Potential Hessdalen-Type Sites in the World

How many Hessdalen-type sites simultaneously exist in the world? By following our previous reasoning, the central wormhole (with an assumed power ~ 1GW) can feed 1000 BBL "tanks" (power ~ 1MW). In reality, there are fewer than 1000 Hessdalen sites in the world; instead, the number of Hessdalen sites is of the order of tens (Te-

odorani, 2004, 2014). However, most of these sites are inactive, and only a few of them are active. The analogy with volcanism can help us understand the situation. How many volcanoes are there in the world? Although volcanologists have no set rules for defining an active volcano, there are approximately 1500 potentially active volcanoes worldwide. However, most of these volcanoes can be dormant for lengthy periods. How long does it take to erupt a dormant volcano? A simple response is that dormant volcanoes are waiting until conditions are right to erupt. There are approximately 100 volcanoes actively erupting each year in the world (following the Global Volcanism Program at the Smithsonian Institution, see Siebert et al., 2010). By a very crude comparison, this may be the number of BBL sites that are active in the world each year. Let us note, however, that even though tectonic activity and BBL phenomena are considered fully independent in the present paper, some geological studies instead claim that many BBL sightings have been seen around volcanoes or other tectonically active areas (Bach, 1993; Thériault et al., 2014; Straser, 2016). In any way, if it's actual, this alleged non-accidental correspondence between tectonic activity and BBLs needs to be confirmed.

Photoionization Model for Hessdalen Lights

The power of a BBL reaches values up to 19 kW (Teodorani, 2004). Before division, the energy source of the seed exiting the soil is assumed to be supplied by the mouth of a wormhole located at its center of this seed. By adapting the power $P_{WH} = P_{BBL} = 10$ kW and with the temperature $T_{WH} = T_S \, 10^7 \, K$ (T_S is the temperature estimated by the solar models at the center of the Sun) of the wormhole, we obtain the radius of the wormhole mouth:

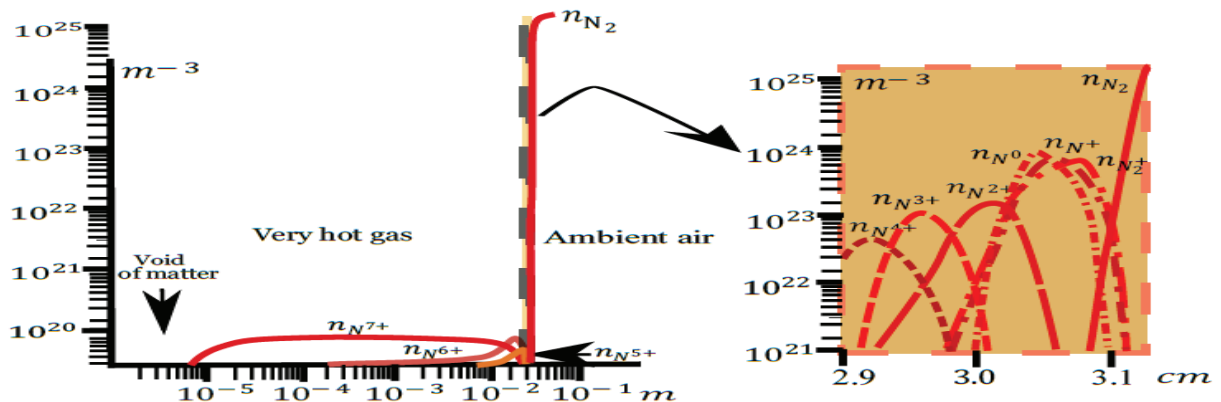$$R_{WH} = 10^{-9} \ m \qquad (4)$$

Figure 8. Structure of a BBL Seed

The source of energy of a mean seed exiting the soil can eventually be an insignificant object of nanometric size.[4].

A temperature of 10^7 K is indeed very high, and the radiation pressure at the mouth of the wormhole hole is $\sim 2.52 \times 10^{12}$ $N\,m^{-2}$. The net effect is to push back the atmospheric gas and create a very small cavity, i.e., a void of matter surrounding the wormhole[5]. This very small cavity is full of radiation at very high temperature[6]. However, around the mouth of the wormhole, the mean radiation temperature decreases as the inverse of the square root of the radius r . Then, beyond a very short distance of 10 μm, the radiation pressure is much lower than the atmospheric pressure ($P_a = 10^5$ $N\,m^{-2}$). The method of calculations has been presented in a previous paper (Pascoli, 2021), and the panel of formulae will not be again fully incorporated. However, we add some complements given that the temperature T_{WH} of the mouth of the wormhole and the ionization degrees of the nitrogen atoms are much higher.

The total recombination rate coefficients $\alpha(i)$ for the transitions $i + 1 \rightarrow i$, where i expresses the ionization degree (i varies from 0 to 6 for the nitrogen atom), are issued from Péquignot et al. (1991). The molecular recombination coefficients $\alpha_D(i)$ are taken from Tamadate et al. (2020). For the photoionization cross sections of the atomic N and its ions, we have chosen a well-known and easily handled law for the species :

$$\sigma_{1,v}(i) = 10^{-22}\left[\alpha\left(\frac{v_i}{v}\right)^s + (1-\alpha)\left(\frac{v_i}{v}\right)^{s+1}\right] \quad m^2 \tag{5}$$

Where α and s are coefficients that are supplied in the paper by Henry (1970), and v_i are the threshold wavelengths in Table 2 (see also Osterbrock and Ferland, 2005). We dispose of many refined calculations for photoionization cross sections (Brumboiu, Eriksson, & Norman, 2019 and references therein); however, the theoretical data must be fitted, and the results cannot easily be manipulated. In any case, for energies of approximately 10–100 eV, the photoionization cross sections are typically of the order of one megabarn or 10^{-22} m^2 Thus, given that the list of photoionization cross sections is still not complete for high degrees of ionization, we have chosen to fix $\alpha = 3$ and $s = 2.5$ when $i \geq 3$ in Eq. 5.

For molecular nitrogen N_2 we fit published tabulated values using the downloading link https://home.strw. leidenuniv.nl/~ewine/photo. A counterpart curve has been used for the corresponding mono-cation.

The equation system, already presented in the preceding paper (Pascoli, 2021), has been completed by the data supplied just above; then it has been normalized and solved by an iterative method at each point of radius r (the zero of r is taken at the wormhole mouth). MATLAB numerical software is used throughout the calculations. This software has been implemented on the MatriCS calculation platform at UPJV to date. The results are displayed in Fig. 8.

Let us note that the seed is not a full object with a diffuse aspect; it is instead a sharp-edged hollow ball filled with a very hot and very low-density gas. A quick rule of thumb for the calculation of the Strömgren radius of the seed can be made. The spectral radiant emittance of a black body is provided by the following relationship:

$$M_v = \frac{2\pi h \frac{v^3}{c^2}}{\exp\frac{hv}{kT_{WH}} - 1} \tag{6}$$

Table 2 Threshold Frequencies and Wavelengths for the Ionization Degrees of the Nitrogen Atom (NIST Atomic Spectra Database. Last update to data content: October 2022).

Ion	Charge i	Ground Shells	Ground Level	Ionization Level	Ionization Energy (Ev)	Frequency (Hz)	Wavelengths (nm)
N I	0	$1s^2 2s^2 2p^3$	$^4S^0_{3/2}$	$2p^2\ ^3P_0$	14.53	3.5×10^{15}	85.7
N II	+1	$1s^2 2s^2 2p^2$	$^3P_0$	$2p\ P^0_{1/2}$	29.60	7.1×10^{15}	41.9
N III	+2	$1s^2 2s^2 2p$	$P_{1/2}$	$2s^2\ ^1S_0$	47.44	1.1×10^{16}	27.0
N IV	+3	$1s^2 2s^2$	$^1S_0$	$2s\ ^2S_{1/2}$	77.47	1.8×10^{16}	16.5
N V	+4	$1s^2 2s$	$^2S_{1/2}$	$1s^2\ ^1S_0$	97.89	2.3×10^{16}	12.9
N VI	+5	$1s^2$	$^1S_0$	$1s\ ^2S_{1/2}$	552.07	1.3×10^{17}	2.3
N VII	+6	$1s$	$^2S_{1/2}$		667.05	1.6×10^{17}	1.9

Then, for the photon flux at the mouth of the wormhole, we obtain the following equation:

$$\mathcal{N}_{ph} = 4\pi R_{WH}^2 \int_{v_{i=6}}^{\infty} dv \, \frac{M_v}{hv} \tag{7}$$

It is found that $N_{ph} \sim 1.3 \; 10^{19}$ ph s^{-1} With the electronic density $n_e \sim 7n_{N^{7+}} \sim 9 \; 10^{19}$ m^{-3}, a rough estimate of the Strömgren radius is as follows:

$$R_S = \left(\frac{3\mathcal{N}_{ph}}{4\pi\alpha_{N7}+n_e^2}\right)^{\frac{1}{3}} \gtrsim 1 \, cm \tag{8}$$

As in the preceding paper, relative to the topic of Hessdalen lights, we find a seed of centimetric radius.[7] This seed is composed of a quasi-hollow bubble with a weak density, $n_{N7+} \sim 9 \; 10^{19}$ m^{-3}, and a very high temperature of 10^7 K This temperature appears impressive; however, the energy contained in the bubble is very weak ~1 J. This energy instantaneously dissipates within ~10^{-4} s without the energy input from the wormhole mouth (power 10 kW). A similar result was found in a previous paper (Pascoli, 2021). Let us notice that this very hot bubble is hidden from the view of the observer by an ionized shell, approximately one millimeter thick, with mean densities varying from approximately 4 10^{23} to 2 10^{24} m (**PER AUTHOR NOTE: SPECIFICITY FOR WHERE -3 GOES**)and mean temperatures varying from approximately 10^4 K to 2 10^3

K from the inside to the outside. This is inside this thin shell, assimilated to a black body, that the visible spectrum is produced with variable colors. The energy stored in this envelope is ~1 J.

Dynamics of the Ionized Envelope

It is interesting to study the dynamics of the ionized shell. A series of equations must be considered:
- The dynamic equation for a spherical envelope:

$$\frac{d}{dt}\left(M_{env}\frac{dR}{dt}\right) = 4\pi \left[R^2 P_i - (R + \Delta R)^2 P_a\right] \tag{9}$$
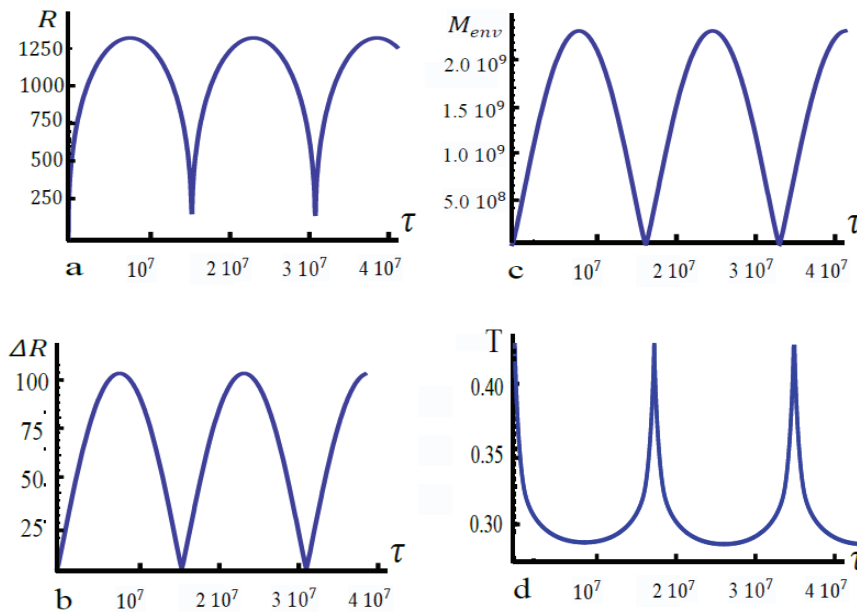
Where M_{env} is the mass of the envelope, $Pa = 10^5$ is the atmospheric pressure, P_i is the internal pressure within the very hot bubble, R is the mean radius, and ΔR is the thickness of the envelope. By assuming that $\Delta R << R$ (thin shell approximation), the equation transforms as follows:

$$\frac{d}{dt}\left(M_{env}\frac{dR}{dt}\right) = 4\pi R^2 (P_i - P_a) \tag{10}$$

$$\frac{dM_e}{dt} = 4\pi R^2 \rho_a \left(1 - \frac{1}{2}\left(\frac{R(0)}{R(t)}\right)^{\frac{3}{2}}\right)\frac{dR}{dt} \tag{11}$$

- Thickness

$$\Delta R = \frac{M_{env}}{4\pi R^2 \rho_{env}} \tag{12}$$

Note. Fig. 9 a displays the mean radius of the shell (unit reference = 1.8 10^{-5} m), Fig. 9 b displays the thickness of the shell (unit reference = 1.8 10^{-5} m), Fig. 9 c shows the mass of the shell (unit reference = 2.4 10^{-14} kg) and Fig. 9 d shows the mean temperature of the shell (unit reference = 10^4 K).

Figure 9. Pulsating BBL
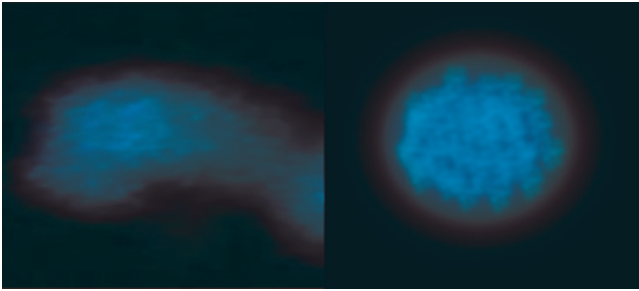
Note. Left: BBL (E. Strand, Hessdalen.org); right: multimouth wormhole model.

Figure 10. Visualization of a BBL and its Interpretation.

Where ρ_{env} is the mean density of the envelope. By assimilating the atmosphere to an ideal gas, we obtain the following equation:

$$P_a = \frac{\rho_a}{m_a} k_B T_a \qquad (13)$$

Where ρ_a is the density, T_a is the temperature (T_a = 293 K), and m_a is the mean mass of an air molecule, m_a = 4.8 10^{-23} kg. The plasma in the envelope is essentially a mixture of the dominant species N^0, N^+, N^+_2. Then, the pressure in the envelope is approximately given by the following relationship:

$$P_{env} = \left(n_{N^0} + n_{N^+} + n_{N^+_2} + n_e\right) k_B T_{env} \qquad (14)$$

By assuming the electric neutrality[9], we obtain the following equation:

$$P_{env} = (n_{N^0} + 2n_e) k_B T_{env} \qquad (15)$$

$$T_{env}(0) = 10^4 \ K$$

By considering the results of the preceding paragraph[10], we obtain the following equation:

$$P_{env} \simeq 5 \ n_{N^0} k_B T_{env} = 5 \frac{\rho_{env}}{2 m_a} k_B T_{env} \qquad (16)$$

There are fewer equations than there are unknown variables $M_{env}(t)$, $R(t)$, $\Delta R(t)$ $\rho_{env}(t)$, $T_{env}(t)$, $P_i(t)$, $\rho_i(t)$, and the system is underdetermined. Additionally, other factors based on the results of the detailed model (paragraph 5) must be added.

An analysis of the data in paragraph 5 shows that both the density and the temperature grossly vary in the envelope in a quasi-adiabatic manner, starting from

$$T_{env}(t) = T_{env}(0) \left(\frac{\rho_{env}(t)}{\rho_a}\right)^{\frac{2}{3}} \qquad (17)$$

The gas filling the central cavity is at the temperature T_s This very hot gas forms a bubble (a coronal phase) that
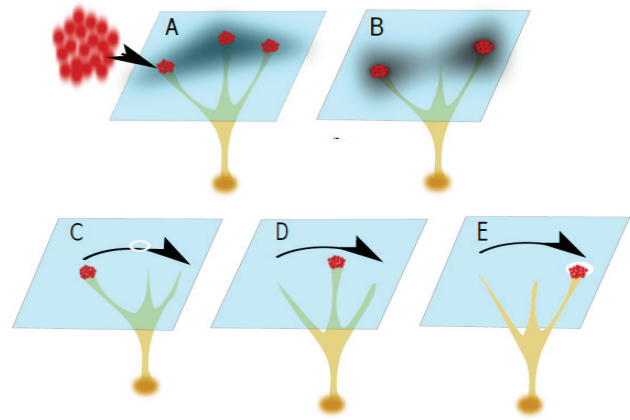
Note. A: triangular configuration; B: dumbbell configuration. The dark area is a contrast effect against the sky background; C, D, E: Three groups of composing elements successively turn on by retraction of the wormhole mouths, simulating an incredibly rapid, even though fictive, "motion" without real translatory displacement of matter (and consequently without violation of the principle of inertia and, obviously, without sonic boom)

Figure 11. Macroscopic Effects Often Described by the Observers.

pushes the envelope with pressure $P_i = 2(x+1) \rho_i/(m_a/2)$ $k_B T_s$, where x = 7 is the highest degree of ionization of the gas ($N_2 \rightarrow 2N^{7+} + 14e^-$). The density ρ_i in this bubble varies according to the following law[11]

$$\rho_i(t) = \rho_i(0) \left(\frac{R(0)}{R(t)}\right)^{\frac{3}{2}} \qquad (18)$$

where $\rho_i(0) = \rho_a$ We solve the system as follows:

$$\frac{d}{dt}\left(M_{env}\frac{dR}{dt}\right) = 4\pi R^2 \left[2(x+1)\frac{T_s}{T_a}\left(\frac{R(0)}{R(t)}\right)^{\frac{3}{2}} - 1\right] P_a \qquad (19)$$

$$\frac{dM_{env}}{dt} = 4\pi R^2 \rho_a \left(1 - \frac{1}{2}\left(\frac{R(0)}{R(t)}\right)^{\frac{3}{2}}\right)\frac{dR}{dt} \qquad (20)$$

Eq. 12 is applied to determine the thickness. The initial conditions are $\rho_i(0) = \rho_e(0) = \rho_a$, $m(0) = 0$

We apply $t = R(0) / C_s \tau$, where $c_s = \sqrt{\gamma Z k_B T_s/m_N}$ (γ is the adiabatic index and Z the charge state), $R(t) = R(0) u(t)$, with $R(0) = 1.8 \ 10^{-5}$ m, and $M_{env}(t) = 4\pi/3\rho_a R(0)^3 m(t)$, and $4\pi/3\rho_a R(0)^3 = 2.14 \ 10^{-14}$ kg, with The variables τ, μ, and m are three dimensionless variables.

Eventually, the dimensionless governing equations are as follows:

$$\frac{d}{d\tau}\left(m\frac{du}{d\tau}\right) = au^2\left[\frac{b}{u^{\frac{3}{2}}} - 1\right] \qquad (21)$$

$$\frac{dm}{d\tau} = 3u^2\left(1 - \frac{1}{2}\frac{1}{u^{\frac{3}{2}}}\right)\frac{du}{d\tau} \qquad (22)$$

Table 3. Hypothesized Composition of a BBL.

Number of Composing Elements in a One-Meter BBL	Power (W) by Composing Element	Size of a Composing Element	Size of the Ionized Region Surrounding a Composing Element	Steric Occupation of the Plasma Phase
100	100	$10^{-10}\ m$	5 mm	10^{-5}
1000	10	$5\ 10^{-11}\ m$	1 mm	10^{-6}
10 000	1	$10^{-11}\ m$	0.05 mm	10^{-9}

with $a = 3P_a/(\rho_a c_s^2)$ and $b = 4(x+1)T_s/T_a$. The initial conditions are $\rho_i(0) = \rho_{env}(0) = \rho_a$ and $m(0) = 0$, $u(0) = 1$, $^{du}/_{dt}(0) = 0$ and A numerical calculation gives $a = 4.6\ 10^{-6}$ and $b = 9.6\ 10^5$. The results are displayed in Fig. 9.

We note that the seed does not have a constant radius, and it periodically oscillates as a function of time. The period is ~ $5\ 10^{-4}$ s. This period is very short and could only be visualized with a high-speed video camera. In particular, the variation in temperature between 10^4 and $3000\ K$ (Fig. 9d) must lead to a variation in color from the blue-white to the red. For instance, in the astrophysics domain, the colors of the stars indicate their surface temperatures. The color is blue-white when the temperature is approximately $10^4\ K$, it is yellow for temperatures of approximately 5000 - 6000 K, and it is orange-red for stars with surface temperatures of approximately $3000\ K$[12]. Proceeding by analogy, and given that the temperature curve is relatively flat (Fig. 9d) and around approximately 3000 K, we can reasonably assume that the tiny seed must appear orange-red immediately after exiting the subsoil. However, the outlet of the subsoil may be rapid, and this phase could be difficult to observe. Then, after multipartitioning of this tiny seed, the ionizing elements are distributed in a very large volume of cold air, and the Rayleigh scattering by the molecules can eventually confer to a BBL a bluish aspect.

BBL Formation

Remarkably, the model here gives a very deceptive small object of centimetric size, itself fed by a nanometric wormhole mouth located at its center, whereas the observed BBLs are sometimes described with a size of a few meters. First, we specify that an HL (or, more generally, a BBL) is not a perfect luminous disk with uniform brightness (Fig. 10).

In Figure 10, we clearly see that the BBL is composed of numerous whitish spots, very likely a hundred or many more. These spots have variable brightness levels and the environmental bluish aspect seems to be due to diffuse radiation produced by cold air molecules.

Then, how do you make a very patchy BBL of one meter in size with a tiny sharp-edged seed, i.e., the small ball of one centimeter in size described in paragraph 5? By considering the instability of this seed, we can imagine it splitting into a multitude of small components, each of them being fed by a point source, i.e., a very small wormhole mouth. In the following, we call composing elements these point sources.[13]. Their size is difficult to estimate; however, we give a table summarizing a panel of sizes (Table 3).

With reference to the steric occupation, we understand why the Hessdalen lights and other BBL-type phenomena are so elusive. A BBL is eventually a metric volume of cold air taken in its molecular form (temperature ~ 293 K), including a swarm of very tiny ionized regions ~ 1 mm inside it (range of temperatures~ $2\ 10^2$ - $10^4\ K$) . We have then the image of a plum pudding model but with minute grape seeds, corresponding to the ionized fraction (Fig. 10). However, the BBL is continuously fed by a swarm of composing elements in it, and the power globally emitted by the BBL is high ~ 10 kW (maybe ~ 100 kW in a few cases). When the swarm of wormholes retracts outside of space in totality after a relatively long period, of the order of a few seconds or minutes, the source of energy suddenly shuts down; the BBL turns off very rapidly, within **10^{-4} - 10^{-3}**, leaving no trace. Conversely, if the totality or part of the swarm of composing elements reappears, the BBL quasi-instantaneously turns on with changing forms. If the phenomenon repeats periodically, we see a flashing BBL with changing colors. Notably, this second period, of the order of a few seconds or minutes, is easily perceptible by the observer; it occurs mainly due to the successive retractions and reappearance of wormhole mouths in the atmosphere. Groups of composing elements can turn back independently, leading to various effects producing different impressive geometric shapes (Fig. 11).

Approaching a BBL

A spherical BBL with a radius of 1 m has an area of 12 m^2. The area of a hand is approximately 10 cm x 10 cm = 10^{-2} m^2. With an isotropic power of 10 kW for a mean BBL, the power received by a hand directly at the surface of the BBL is 10 W. The solar energy that reaches the Earth at sea level is roughly 1000 W m^{-2} or 10 W over an area of a hand. The values are identical (10 W). This phenomenon is a direct indication of the sensation that can be felt by touching a one-meter BBL with a mean power of 10 kW. As an illustration, a one-meter BBL has been seen lying on snowy ground without any traces of snow thawing after its disappearance (Nikitin *et al.,* 2018). The larger a BBL is, the less dangerous it is, even though it is not an intangible rule. BBLs can be dangerous if the power is larger than 10 kW, as assumed in some cases (Maccabee, 1996, referenced in Sturrocks, 1998). Conversely, for the same power, a one-centimeter BBL (for instance, the seed emerging from the BBL "tank" at the very beginning of the process before division) can trigger a fire in a house. Fortunately, according to the FAO Global Land Cover Share database, only 0.6% of Earth's land surface is defined as artificial cover, such as construction. Moreover, a BBL is an extremely rare phenomenon, and the probability that a one-centimeter BBL goes from the subsoil to the atmosphere by crossing a residential building is very weak.[14].

Absence of a Sonic Boom

Another aspect of the HL phenomena is the absence of a sonic boom when the BBL moves with a supersonic velocity. First, the term "move" associated with the BBL poorly describes the phenomenon. In reality, whereas the swarm of point sources (composing elements) moves, the small volume of ionized air surrounding each composing element does not move. The air is ionized on the spot and renewed continuously around each composing element. This effect simulates an apparent translatory motion without real displacement of atmospheric matter. This may be the key to why no sonic boom is heard. Thus, a BBL is a phenomenon, not a definite object (or, following the terminology, an unidentified aerial phenomenon (UAP) rather than an unidentified flying object (UFO), even though the swarm of composing elements contained in it can be assimilated to an "object").

However, another motion is real, which is the oscillation of the ionized shell surrounding each composing element. By following the results presented in paragraph 6, this ionized shell (thickness < 1 mm) surrounding each composing element (size ~ 5 10^{-11} m) oscillates. Part of the energy of the oscillatory motion is very likely dissipated in the form of shock waves. However, a shock wave pro-duces a sonic boom. This finding seems to be contrary to what we said above. Eventually, it is difficult to escape to a sonic boom. How can this problem be solved?

A ballistic crack of a supersonic small bullet (size ~ 1 cm) is characterized by a frequency that is much higher than that of a bang of a supersonic fighter jet (size ~ a few meters). Obviously, the frequency spectra of a sonic boom or a ballistic crack are strongly dependent on the velocity and shape of the object. However, very crudely, the mean characteristic frequency of a supersonic object is grossly equal to the inverse of its size. The audible frequencies of the sonic boom of a fighter jet are approximately 100 Hz (even with a very large band of frequencies around this mean value); for a small bullet, the mean frequency is approximately 10 kHz. We can reasonably assume that the frequencies of a supersonic object that is approximately one-millimeter peak at approximately 100 kHz. Then, it is possible that the acoustic frequencies emitted by the oscillation of the ionized envelope (size ~ 1 mm) surrounding each composing element are located in the ultrasonic domain and are thus inaudible to humans. In addition, the range of ultrasounds in the air is smaller than the range of audible sounds, even though the attenuation considerably depends on the properties of the gas medium: temperature, pressure, and humidity (Vladišauskas & Jakevičius, 2005). As a result, the intensity of ultrasounds emitted by a tiny oscillating envelope can substantially be weakened before the reception by any device. Nevertheless, it would be most interesting to install an ultrasonic sensor on the Hessdalen site to know if this type of wave is emitted (or not) by the BBLs. For the model proposed in this paper, the aim of these measurements is to fix the size of the composing elements and to estimate their number in a one-meter BBL for a power of 10 kW. Clearly, the analysis will be complex due to the interferences between the various shock waves produced by a multitude of small oscillating sources; however, it can be an interesting topic.

DISCUSSION

After the works of Strand, Hauge, and a few other researchers and the seminal paper by Teodorani (2004), we know that the Hessdalen lights and other BBLs of sizes of ~ 1 - 10 m seen around the world can naturally be studied by physics. We have attempted to follow this path in this paper. By following the scenario described here, a BBL with a size of ~ 1 - 10 m is essentially a volume of air at ambient temperature (293 K) and pressure (10^5 Pa). In this volume of cold air, it is assumed that the source of radiation can be a swarm composed of unstable tiny wormhole mouths of sizes of ~ 10^{-10} - 10^{-11} m ; each of these mouths

feeds a small ionized region of 1 *mm* in size. The thin shell surrounding each of these pulsating ionized regions has a mean temperature of 2500 - 3000 *K* at its maximum extension. In addition, the composing elements of the swarm of wormhole mouths are not independent; their relative positions are strongly correlated because they are linked to a "tank" (itself a wormhole of a size of ~10^{-8} *m*) located deep in the subsoil of the site under question (for instance, the Hessdalen valley). The model predicts that 1000 Hessdalen-type sites may exist in the world with a low proportion of active sites at the same moment (by analogy with volcanism).

The first item of importance of the model is to advance the physics of BBLs:

i. The production and analysis of spectra, which have already begun, must be continued. Two types of HLs are predicted by the model: HLs composed of only air molecules (resulting from an extradimensional transition between the HL (BBL) "tank" in the subsoil and atmosphere) and HLs composed of a mixture of cold air molecules and silicon particles (resulting from a three-dimensional transition between the subsoil and atmosphere). In the first situation, spectra of N^2 and O^2 molecules only appear, and in the second situation, the spectra of silicon or other terrestrial elements (scandium, for instance) must be present.

ii. The detection of a monopolar magnetic field would be direct proof of the existence of a wormhole, as already proposed in a preceding paper (Pascoli, 2021). Notably, the presence of a monopolar magnetic field can explain the division of the initial seed, originating from the subsoil, into an aerial swarm of subnanometric wormholes over a large extension (~ 1 *m*) because monopolar magnetic fields of the same polarity repel one another. It will be interesting to conduct a theoretical study to investigate this topic.

iii. Measurements must be performed concerning the production of ultrasonic waves, which are possibly emitted by the BBLs; these measurements made it possible to estimate the sizes of the entities composing the swarm of subnanometric wormholes. The signature of a BBL could be a series of cracks in the ultrasonic domain. This signature would allow us to immediately discriminate between true BBLs and other misinterpretations (planet, headlight, etc.). In addition, ultrasonic signal measurements may be easier to realize than the obtention of very high-resolution optical spectra.

iv. We know from geophysics that the acquisition of thermal datasets allows the detection of enhanced geothermal flow in a localized region. Due to the in-

ferred presence of a BBL "tank" deep in the subsoil under the Hessdalen valley, the geothermal gradient can be somewhat higher than that in the nearby valleys. The temperature of subsoil over a few meters under the surface results almost entirely from heating by the Sun and cooling through radiation; for this reason, a shallow exploratory drill hole of a few meters would prove to be totally ineffective. Also, highlighting an anomalous geothermal gradient under the Hessdalen Valley must require drilling a borehole deeper than a few hundred meters. Various mechanized drilling techniques are operative, and several highly experienced borehole drilling companies can easily make it, though unfortunately, at high costs (with minimal values of approximately 10,000 dollars for 100 meters, depending on ground properties, knowing that a minimum of four or five boreholes, one in the Hessdalen valley and the other ones in the nearby valleys, are needed). Let us note once again that the fact that the Hessdalen lights appear in the Hessdalen valley and not in the nearby valleys clearly indicates that the source of the phenomenon hidden in the subsoil must nonetheless be relatively close to the surface. In any case, if we want to solve the puzzle of the Hessdalen light phenomena, we must give ourselves the means to do so.

The second and very important item would be to confirm the existence of planetary wormholes. Galactic wormholes of size ~ 10 *AU* and stellar wormholes of kilometric size have recently been predicted. However, these seemingly elusive entities could be closer to home as one might think about them, even though they have a much smaller size. The discovery of planetary wormholes of micrometric-nanometric size would be a major breakthrough in the wormhole domain. Even though entirely speculative for the time being, the present idea could simultaneously solve the BBL enigma and eventually prove the reality of stable wormholes in the Universe. One last question: What is the probability that wormholes are at the origin of the HL phenomena? Maybe we can believe that this probability is very thin, but in reality, a belief has nothing to do with science. The true referee in science is experimentation. Only and only experimentation can validate an idea in physics, no matter how weird it sounds. Also, we should leave no avenues unexplored in order to understand the BBL phenomena.

ACKNOWLEDGMENTS

ENDNOTES

[1] The interest in the proposal of wormholes against black holes in the field of astrophysics and related domains is that black holes have a troublesome central singularity, whereas wormholes do not. Thus, a traversable wormhole has no horizon and allows an extradimensional passage through it. However, this implies that, in the strict context of general relativity, a violation of the weak energy condition must unavoidably occur when passing the throat of the wormhole. On the other hand, it is known that certain wormhole solutions, which have been constructed using various modified theories of gravity, do not require weak energy conditions violating matter. Unfortunately, this important point is not definitely fixed in the models (Roman, 1988; Frolov & Novikov, 1998; Lobo, 2018).

[2] Concerning now the complex issues related to the stability and the crossing of the wormholes, these are items largely debated today and are still inconclusive (Konoplya & Zhidenko, 2022). It is a continuing challenge that applies to both the families of galactic and stellar wormholes. Unfortunately, no solution can be supplied in the strict framework of the general relativity for which all wormholes are definitively unstable. We need a quantum gravity theory to solve this complex inquiry. On the other hand, the estimation of the gravitational mass of the wormhole has been made above in the framework of general relativity. In reality, other forces (for instance, the Casimir force, even though this one is limited to the quantum level) necessarily compensate for the gravitational force; otherwise, we know the wormhole will instantaneously collapse. In this case, the gravitational potential at the mouth of the wormhole does not slowly vary as $1/r$; in contrast, it is very likely screened, and then, it rather strongly decreases as $1/r \; e^{-r/rD}$, where the constant plays the role of a gravitational Debye radius (maybe $r_D \sim 10^{-9} \; m$ for a nanometric wormhole). This type of gravity is related to modified gravity theories, which have already tentatively been applied to other fields of astrophysics, especially in the very large-scale domain (see Moffat, 2008), where a Yukawa-type potential is assumed. However, we know that modified gravity can lead to nonstandard yet traversable wormhole geometries that are fundamentally different from their unstable counterparts in general relativity. Unfortunately, modified gravity theories are overabundant and are facing various mathematical challenges. Hence, the theories of wormholes appear in the early stages of development. We must mention that the experimental point of view has been completely neglected in all these theoretical studies. However, without experimental support, a theory cannot be fully validated and even appears irrelevant. In contrast, if the HL and BBL phenomena have any interrelationship with the wormholes as hypothesized in this paper, the study of HLs or BBLs would constitute a formidable experimental field of investigation for the wormholes.

[3] Spectra of a few BBLs have been obtained (Teodorani et al., 2001; Hauge, 2007). The presence of elements like N, O and, Si, Ca, and Mg has been effectively suspected, but unfortunately, the too low-resolution of these spectra forbids a really reliable spectrochemical identification.

[4] In the preceding paper (Pascoli, 2021), a size of 50 μm was found, but the wormhole temperature was then assumed to be much lower $\sim 10^5 \; K$.

[5] The gas of the atmosphere is strongly pushed aside by the intense radiation stemming from the wormhole mouth and consequently cannot penetrate the wormhole. In this work, the wormhole is a canal for the radiation field, not for the matter. Consequently, a cavity devoid of matter appears surrounding the wormhole mouth (Fig. 8).

[6] We recall the formula of the radiation pressure for a black body P_{rad} = $1/3 \; aT^4$ a where a is the radiation constant, a = 7.57 $10^{-16} \; J \; m^{-3} \; K^{-4}$.

[7] By taking T_{WH} = $10^7 \; K$ for a power of 100 kW , we obtain a radius multiplied by 3, and for a power of 1 MW, we obtain a radius multiplied by 10.

[8] Cf. note 10.

[9] By imposing the electric neutrality, we have the following condition: $n_e = n_{N+} + n_{N2+}$.

[10] By considering the results of the simulation presented in Fig. 8, we have $n_e \sim n_{N+} \sim n_{N2+}$ The mean density in the envelope ρ_{env} (m_a is the mean mass of an air molecule) can be simply expressed as follows:

$$\rho_{env} = n_{N^0} m_{N^0} + n_{N^+} m_{N^+} + n_{N_2^+} m_{N_2^+}$$

$$\simeq n_{N^0} m_{N^0} + n_{N^0} m_{N^0} + n_{N^0}(2m_{N^0})$$

$$= 4n_{N^0} m_{N^0} = 2n_{N^0} m_a$$

This equation is indeed a very crude approximation that is sufficient for our purpose.

[11] ρ_i varies as $R^{3/2}$ and

$$M_i(t) = \frac{4\pi}{3} \rho_i(0)[R(0)R(t)]^{\frac{3}{2}}$$

This equation results from the fact that the mass of the hot bubble (coronal phase) is not constant; instead, it increases at the expense of the thin shell, which erodes on its inner face.

[12]   To the naked eye, all the stars appear white because they are too dim for the human eye to perceive color. In any way, the color restitution depends on the sensibility of the image sensor.

[13]   These composing elements are also wormhole mouths but of a size much smaller than 10^{-9} m.

[14]   In contrast, ordinary ball lighting observed sometimes in a house seems to have a very weak power of the order of a few watts; they consequently do not produce any damage. Very likely, the BBLs described in this paper and the ordinary ball lighting are very different phenomena.

REFERENCES

Bach, E.W. (1993). *Ufos from volcanoes*. Tenafly, New Jersey: Hermitage Publishers.

Bakopoulos, A., Charmousis, C., & Kanti, P. (2022). Traversable wormholes in beyond Horndeski theorie. *JCAP*, *05*, 22-59. https://doi.org/10.1088/1475-7516/2022/05/022

Blazquez-Salcedo, J., Knoll, C., & Radu, E. (2021). Traversable wormholes in Einstein-Dirac-Maxwell theory. *Phys. Rev. Lett.*, *126*(10), Article 101102. https://doi.org/10.1103/PhysRevLett.126.101102

Brumboiu, I.E., Eriksson, O., & Norman, P. (2019). Atomic photoionization cross sections beyond the electric dipole approximation. . *J. Chem. Phys.*, *150*, Article 044306. https://doi.org/10.1063/1.5083649

Dai, D.C., & Stojkovic, D. (2019). Observing a wormhole. *Phys. Rev. D*, *100*, Article 083513. https://doi.org/10.1103/PhysRevD.100.083513

Dai, D.C., & Stojkovic, D. (2020). Response to the comment on "Observing a wormhole" . *Phys. Rev. D*, *101*, Article 068302. https://doi.org/10.1103/PhysRevD.101.068302

Das, P., & Kalam, M. (2022). Wormhole in the Milky Way galaxy with global monopole charge. *The European Physical Journal C*, *82*, 342. https://doi.org/10.1140/epjc/s10052-022-10322-z

Davies, J.H., & Davies, D.R. (2010). Earth's surface heat flux. *Solid Earth*, *1*(1), 5–24. https://doi.org/10.5194/se-1-5-2010

Dye, S.T. (2012). Geoneutrinos and the radioactive power of the Earth. *Reviews of Geophysics*, *50*(3). https://doi.org/10.1029/2012RG000400

Dzhunushaliev, V., Folomeev, V., Kleihaus, B., & Kunz, J. (2011, April 26). A star harbouring a wormhole at its core. *Journal of Cosmology and Astroparticle Physics*, *04*, 031. https://doi.org/10.1088/1475-7516/2011/04/031

Emparan, R., Grado-White, B.D., Marolf, D., & Tomasevic, M. (2021). Multi-mouth traversable wormholes. *JHEP*, *05*, 032. arXiv:2012.07821v2 https://doi.org/10.1007/JHEP05(2021)032

Frolov, V., & Novikov, I. (1998). *Black hole physics: Basic concepts and new developments*. Springer. https://doi.org/10.1007/978-94-011-5139-9

Fuchs, S., et al. (2021). The Global Heat Flow Database: Release 2021. https://doi.org/10.5880/fidgeo.2021.014

Gao, P., D.L., & Wall, A.C. (2017). Traversable wormholes via a double trace deformation. *Journal of High Energy Physics*, *151*, 2017-2041. https://doi.org/10.1007/JHEP12(2017)151

Henry, R.J.W. (1970). Photoionization cross-sections for atoms and ions of carbon, nitrogen, oxygen, and neon. *The Astrophysical Journal*, *161*, 1153–1155. https://doi.org/10.1086/150615

Hauge, B.G.,Montebugnoli, S. (2012). Different states of the transient luminous phenomena in Hessdalen valley, Norway. EGU General Assembly 2012, held 22-27 April, 2012 in Vienna, Austria, p.12098 https://ui.adsabs.harvard.edu/abs/2012EGUGA..1412098H/abstract

Iqbal, N., & Ross, S.F. (2022). Towards traversable wormholes from force-free plasmas. *SciPost Phys.*, *12*, 86-107. https://doi.org/10.21468/SciPostPhys.12.3.086

Kirillov, A.A., & Savelova, E.P. (2011). Density perturbations in a gas of wormholes. *Monthly Notices of the Royal Astronomical Society*, *412*(3), 1710–1720. https://doi.org/10.1111/j.1365-2966.2010.18007.x

Konoplya, R.A., & Zhidenko, A. (2022). Traversable Wormholes in General Relativity. *Phys. Rev. Lett.*, *128*, Article 091104. https://doi.org/10.1103/PhysRevLett.128.091104

Krasnikov, S. (2020). Comment on "Observing a wormhole". *Phys. Rev. D*, *101*, Article 068301. https://doi.org/10.1103/PhysRevD.101.068301

Lay, T., Hernlund, J.W., & Buffett, B.A. (2008). Core-mantle boundary heat flow. *Nat. Geosci.*, *1*, 25–32. https://doi.org/10.1038/ngeo.2007.44

Leyton, M.S., & Monroe, J. (2017). Exploring the hidden interior of the Earth with directional neutrino measurements. *Nature Communications*, *8*, Article 15989. https://doi.org/10.1038/ncomms15989

Lobo, F.S.N. (Ed.). (2018). *Wormholes, Warp Drives and Energy Conditions*. Springer International Publishing. ISBN 978-3-319-55182-1

Maldacena, J., & Milekhin, A. (2021). Humanly traversable wormholes. *Phys. Rev. D*, *103*, Article 066007. https://doi.org/10.1103/PhysRevD.103.066007

Moffat, J. (2008). *Reinventing gravity: A physicist goes beyond Einstein*. Thomas Allen Pub.

Morris, M.S., & Thorne, K.S. (1988). Wormholes in space-time and their use for interstellar travel: A tool for teaching general relativity. *Am. J. Phys.*, *56*, 395-412. https://doi.org/10.1119/1.15620

Nikitin, A.I., Bychko, V.L., Nikitina, T.F., Velichko, A.M., & Abakumov, V.I. (2018). Sources and components of ball lightning theory. *J. Phys.: Conf. Ser.*, *996*, Article 012011. https://doi.org/10.1088/1742-6596/996/1/012011

Osterbrock, D.E., & Ferland, G.J. (2005). *Astrophysics of gaseous nebulae and active galactic nuclei*. University Science Books.

Pascoli, G. (2021). Are Hessdalen Lights a Reality, an Illusion, or a Mix of the Two? *Journal of Scientific Exploration*, *35*(3), 590–622. https://doi.org/10.31275/20212171

Pollack, H.N., Hurter, S.J., & Johnson, J.R. (1993). Heat flow from Earth's interior: Analysis of the global data set. *Reviews of Geophysics*, *31*(3), 273. https://doi.org/10.1029/93RG01249

Rahaman, F., Salucci, P., Kuhfittig, P.K.F., Ray, S., & Rahaman, M. (2014). Possible existence of wormholes in the central regions of halos. *Ann. Phys.*, *350*, 561. https://doi.org/10.1016/j.aop.2014.08.003

Roman, T.A. (1988). On the "averaged weak energy condition" and Penrose's singularity theorem. *Phys. Rev. D*, *37*, 546-548. https://doi.org/10.1103/PhysRevD.37.546

Ruedas, T. (2017). Radioactive heat production of six geologically important nuclides. *Geochemistry, Geophysics, Geosystems*, *18*(9), 3269. https://doi.org/10.1002/2017GC006997

Sammon, L.G., & McDonough, W.F. (2022). Quantifying Earth's radiogenic heat budget. *Earth and Planetary Science Letters*, *593*, Article 117684. https://doi.org/10.1016/j.epsl.2022.117684

Siebert, L., Simkin, T., & Kimberly, P. (2010). *Volcanoes of the world* (3rd ed.). University of California Press. ISBN 978-0-520-26877-7.

Straser, V. (2016). VLF electromagnetic signals unrelated to the Central Italy earthquakes occurred between 26 and 30 October 2016, *New Concepts in Global Tectonics Journal*, *4*(3),543-552.

Sturrock, P.A. (1998). Physical evidence related to UFO reports: The proceedings of a workshop held at the Pocantico Conference Center, Tarrytown, New York, September 29 - October 4,1997. *Journal of Scientific Exploration*, *12*(2), 179-229.

Tamadate, T., Higashi, H., Seto, T., & Hogan, C. J. Jr. (2020). Calculation of the ion–ion recombination rate coefficient via a hybrid continuum-molecular dynamics approach. *Journal of Chemical Physics*, *152*(9), 094306. https://doi.org/10.1063/1.5144772

Teodorani, M. (2004). A long-term scientific survey of the Hessdalen Phenomenon. *Journal of Scientific Exploration*, *18*(2), 217–251.

Teodorani, M. (2014). Instrumented monitoring of aerial anomalies: A scientific approach to the investigation on anomalous atmospheric light phenomena. Workshop–CNES (National Center for Space Study)-GEIPAN, Paris, France, July 8–9.

The KamLAND Collaboration (2011). Partial radiogenic heat model for Earth revealed by geoneutrino measurements. *Nature Geoscience*, *4*, 647–651. https://doi.org/10.1038/ngeo1205

Thériault, R., St-Laurent, F., Freund, F. T., & Derr, J. S. (2014). Prevalence of earthquake lights associated with rift environments. *Seismol. Res. Lett.*, *85*(1): 159-178. https://doi.org/10.1785/0220130059

Vladišauskas, A., & Jakevičius, L. (2005). *Ultragarsas, Nr.1*(50). ISSN 1392-2114